Aging and Disease
www.aginganddisease.org
Volume 4, Number 1; 29-37, February 2013

Review

Voxel-based Morphometry of Brain MRI in Normal Aging and Alzheimer's Disease

Hiroshi Matsuda*

Integrative Brain Imaging Center, National Center of Neurology and Psychiatry, Tokyo, Japan

[Received November 12, 2012; Revised November 20, 2012; Accepted December 1, 2012]

ABSTRACT: Voxel-based morphometry (VBM) using structural brain MRI has been widely used for assessment of normal aging and Alzheimer's disease (AD). VBM of MRI data comprises segmentation into gray matter, white matter, and cerebrospinal fluid partitions, anatomical standardization of all the images to the same stereotactic space using linear affine transformation and further non-linear warping, smoothing, and finally performing a statistical analysis. Two techniques for VBM are commonly used, optimized VBM using statistical parametric mapping (SPM) 2 or SPM5 with non-linear warping based on discrete cosine transforms and SPM8 plus non-linear warping based on diffeomorphic anatomical registration using exponentiated Lie algebra (DARTEL). In normal aging, most cortical regions prominently in frontal and insular areas have been reported to show age-related gray matter atrophy. In contrast, specific structures such as amygdala, hippocampus, and thalamus have been reported to be preserved in normal aging. On the other hand, VBM studies have demonstrated progression of atrophy mapping upstream to Braak's stages of neurofibrillary tangle deposition in AD. The earliest atrophy takes place in medial temporal structures. Stand-alone VBM software using SPM8 plus DARTEL running on Windows has been newly developed as an adjunct to the clinical assessment of AD. This software provides a Z-score map as a consequence of comparison of a patient's MRI with a normal database.

Key words: Neuroradiology, MRI, voxel-based morphometry, aging, Alzheimer's disease

Studies of brain morphometry using magnetic resonance imaging (MRI) have been carried out by many researchers as the resolution of an anatomical scan of a whole brain increases with shorter acquisition time. MRI based measures of atrophy are regarded as valid markers of disease state and progression [1]. However, differences in the shape and neuroanatomical configuration of individual brains may cause overlooking of structural differences by visual inspection or volume of interest (VOI) technique. The importance of the voxel-based morphometry (VBM) approach [2] is that it is not biased to one particular structure and gives an even-handed and comprehensive assessment of anatomical differences throughout the brain [3]. MRI data for VBM are acquired as a three-dimensional volumetric T1-weighted image. It has a thin thickness of 1 to 1.5 mm without interslice gap. The image matrix is usually 256X256.

VBM of MRI data comprises segmentation into gray matter, white matter, and cerebrospinal fluid (CSF) partitions, anatomical standardization of all the images to the same stereotactic space using linear affine transformation and further non-linear warping, smoothing, and finally performing a statistical analysis. The output from the method is a statistical parametric map. This review article describes common VBM techniques incorporated in statistical parametric mapping (SPM) software running on Matlab platform and its application to normal aging and Alzheimer's disease (AD). Finally new stand-alone VBM software running on Windows is proposed as an adjunct to the clinical assessment of AD.

***Correspondence should be addressed to:** Hiroshi Matsuda M.D., Integrative Brain Imaging Center, National Center of Neurology and Psychiatry, Tokyo, 187-8551, Japan. Email:matsudah@ncnp.go.jp

ISSN: 2152-5250

Table 1. Voxel-based morphometry studies of age-related changes in regional gray and white matter volumes in the healthy human brain

Study	Study design	VBM method	Age range (Y)	N	Regional changes with advancing age	
					Gray matter volume	White matter volume
Good CD, *et al*. (2001)	cross sectional	optimized VBM (SPM2)	17-79	465	Reduction in parietal, pre-and post-central, insula/frontal operculum, cerebellum, anterior cingulate preservation in medial temporal structures	reduction in frontal, optic radiation, posterior limb of internal capsule, ventrolateral thalamus
Resnick UM, *et al*.(2003)	longitudinal (4 years)	SPM99	59-85	92	Reduction in orbital and inferior frontal, cingulate, insular, inferior parietal	widespread reduction
Matsuda H, *et al*. (2003)	cross sectional	SPM99	18-86	52	Reduction in frontal, temporal, insular cortex, pericentral gyri, and anterior cingulate gyri preservation in medial temporal structures, thalamus, and putamen	
Tisserand DJ, *et al*.(2004)	cross sectional	MNI method	53-84	38	Reduction in frontal, temporal, striate cortex	
Grieve SM, *et al*.(2005)	cross sectional	optimized VBM (SPM2)	8-79	223	Reduction in frontal and parietal cortex preservation in medial temporal structures, thalamus, cingulate gyrus	
Smith CD, *et al*.(2007)	cross sectional	optimized VBM (SPM2)	58-95	122	Reduction in frontal, parietal, temporal	Reduction in anterior corpus callosum
Hutton C, *et al*.(2009)	cross sectional	DARTEL(SPM5)	22-60	48	Reduction in prefrontal, orbitofrontal, temporal regions, insula, cingulate, precentral sulcus	
Curiati PK, et al. (2009)	cross sectional	optimized VBM (SPM2)	67-75	132	Reduction in temporal neocortex, prefrontal cortex, medial temporal region	
Kalpouzos G, *et al*. (2009)	cross sectional	optimized VBM (SPM2)	20-83	45	Reduction in frontal and parietal cortex, insular regions preservation in anterior medial temporal structures, thalamus, brain stem	
Giorgio A, *et al*. (2010)	cross sectional	optimized VBM (FSL)	23-81	66	Reduction in most of cortical regions preservation in occipital pole, caudate nucleus, pallidum, amygdala, hippocampus	Linear reduction in thalamic radiations, anterior limb of the internal capsule, cerebral peduncle, cerebellum, external capsule, nonlinear reduction in superior longitudinal fascicle and superior corona radiata
Giorgio A, *et al*. (2010)	longitudinal (2.5 years)	optimized VBM (FSL)	13-18	24	Reduction in parieto-occipital cortex	Increase in frontal, corpus callosum, retrosplenial, medial parietal cortex
Terribilli D, *et al*. (2011)	cross sectional	optimized VBM (SPM2)	18-50	89	Reduciton in prefrontal cortex and cerebellum preservation in medial temporal region, cingulate gyrus, insular, and temporal neocortex	

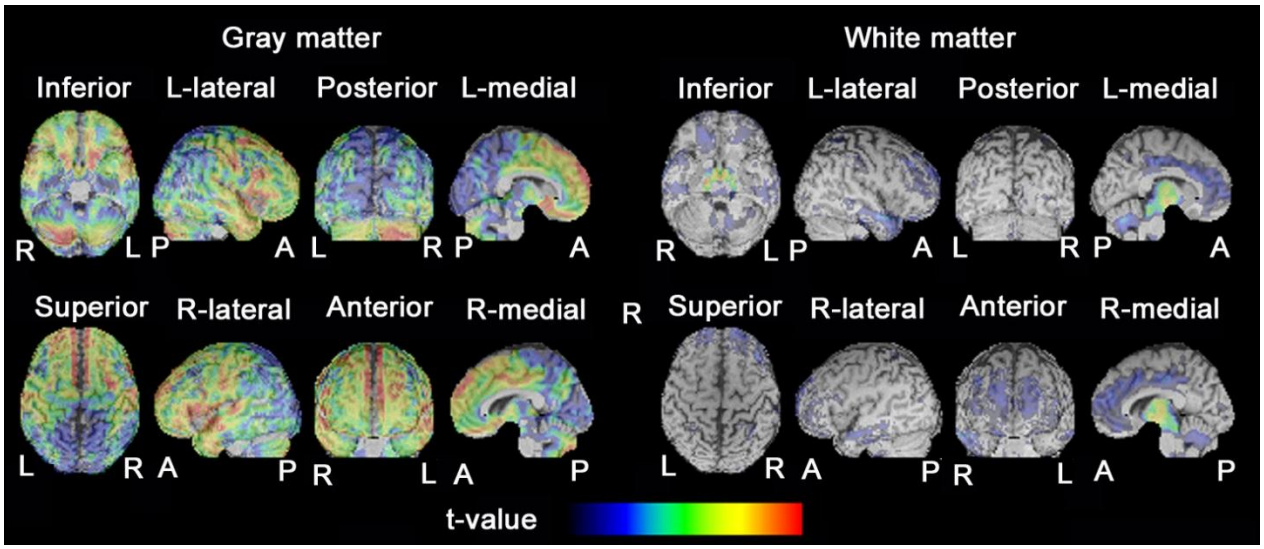

Figure 1. Age-related atrophy in gray and white matter in healthy controls. VBM analysis for 159 healthy volunteers aged from 20 to 74 years showed significant negative correlation of gray matter and white matter volume with advancing age most prominently in frontal cortex and brain stem.

Optimized VBM; This method has been developed for removing areas of missegmented nongray matter voxels by the introduction of additional preprocessing steps to exclude nonbrain voxels prior to anatomical standardization and subsequent segmentation [4,5]. Initial segmentation involves segmentation of the original structural MR images in native space into gray and white matter images, followed by a series of fully automated morphological operations for removing unconnected non-brain voxels in skull, and dural venous sinus from the segmented images. The resulting images are extracted gray and white matter partitions in native space. The extracted segmented gray/white matter images are standardized to the gray/white matter templates, thereby preventing any contribution of nonbrain voxels and affording optimal anatomical standardization of gray/white matter. In order to facilitate an optimal segmentation, the optimized standardization parameters are reapplied to the original, whole brain structural images in native space. The optimally standardized whole brain structural images in stereotactic space are then segmented into gray and white matter, CSF partitions and subject to a second extraction of standardized segmented gray/white matter images. The brain extraction step is repeated at this stage because some nonbrain voxels from scalp, skull, or venous sinuses in the optimally normalized whole brain images could still remain outside the brain margins on segmented gray/white matter images.

As a result of nonlinear spatial normalization based on discrete cosine transforms, the volumes of certain brain regions may grow, whereas others may shrink. In order to preserve the volume of a particular tissue within a voxel, a further processing step is incorporated. This involves multiplying (or modulating) voxel values in the segmented images by the Jacobian determinants derived from the anatomical standardization step. In effect, an analysis of modulated data tests for regional differences in the absolute amount (volume) of gray matter, whereas analysis of unmodulated data tests for regional differences in the concentration of gray matter. Finally, each optimally standardized, segmented, modulated image is smoothed by convolving with an isotropic Gaussian kernel with 12-mm full width at half maximum (FWHM). The smoothing step helps to compensate for the inexact nature of the anatomical standardization. Moreover it has the effect of rendering the data more normally distributed, increasing the validity of parametric statistical tests.

SPM8 plus diffeomorphic anatomical registration using exponentiated Lie algebra (DARTEL); DARTEL incorporated in SPM8 is an implemented algorithm for diffeomorphic image registration [6]. It has been formulated to include an option for estimating inverse consistent deformations. This nonlinear registration is considered as a local optimization problem, which is solved using a Levenberg–Marquardt strategy. A constant Eulerian velocity framework is used, which allows a rapid scaling and squaring method to be used in the computations. This technique improves inter-subject registration. VBM8 toolbox (http://dbm.neuro.uni-jena.de/vbm8/) is available for VBM using SPM8 plus DARTEL for both cross-sectional and longitudinal studies.

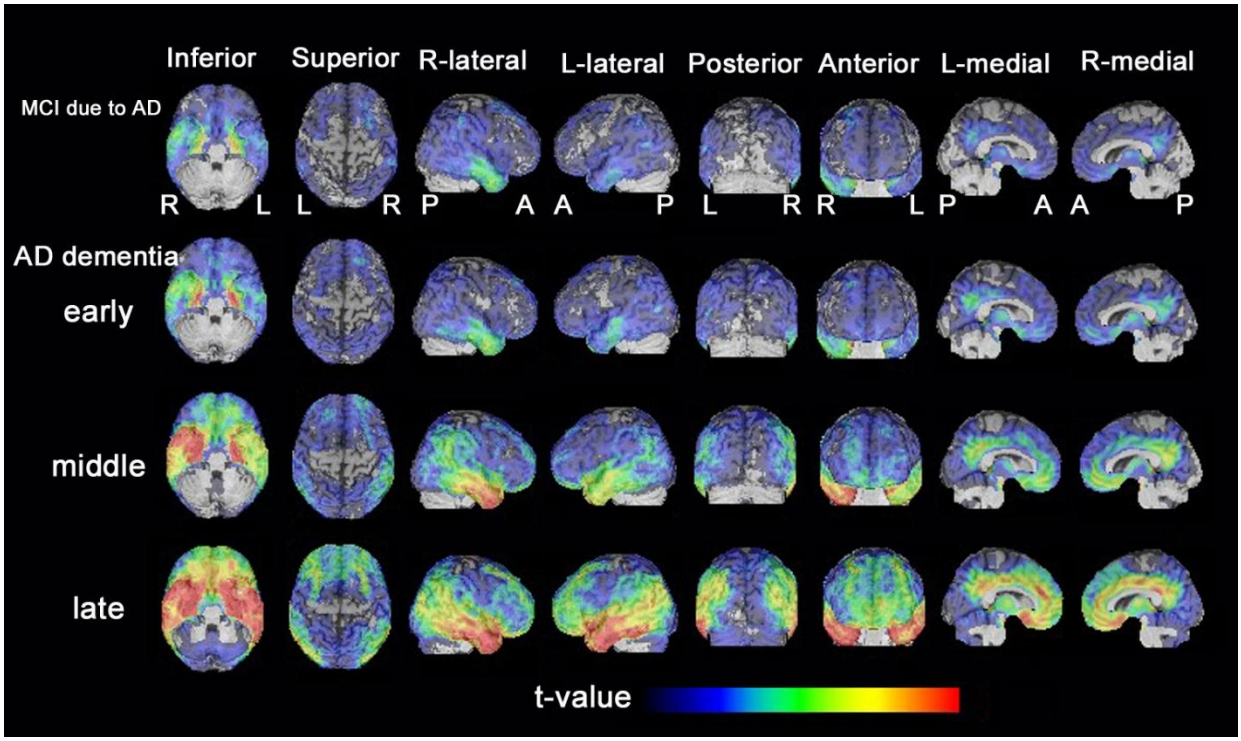

Figure 2. Gray matter atrophy associated with progress of AD. VBM analysis showed significant atrophy initially in medial temporal structures at the stage of mild cognitive impairment (MCI). As AD progresses, atrophy of medial temporal structures becomes more prominent. Moreover atrophy extends into lateral temporal cortex, parietal and frontal association cortex, and posterior cingulate gyrus and precuneus. Peri-central and occipital cortex and cerebellum are spared atrophy. Groups of MCI due to AD, early AD, middle AD, and late AD comprise 61, 42, 49, and 26 subjects, respectively.

In the SPM8 plus DARTEL procedure, T1-weighted images were classified into gray matter, white matter and CSF using the segmentation routine implemented in SPM8, that gives both the native space versions and DARTEL imported versions of the tissues. SPM8 and VBM8 toolbox provides better segmentation accuracy and reliability than FMRIB's Software Library and FreeSurfer software programs [7]. The DARTEL imported versions of gray and white matter were used to generate the flow fields (which encode the shapes), and a series of template images by running 'DARTEL (create templates)' routine. During this step, DARTEL increases the accuracy of inter-subject alignment by modeling the shape of each brain using millions of parameters. DARTEL works by aligning gray matter among the images, while simultaneously aligning white matter. This is achieved by generating increasingly crisp average template data, to which the data are iteratively aligned. The flow fields and final template image created in the previous step are used to generate smoothed (8-mm FWHM), modulated, spatially normalized and Jacobian scaled gray and white matter images resliced to isotropic voxel size in Montreal Neurological Institute space. DARTEL provides better registration accuracy than other widely used nonlinear deformation algorithms including optimized VBM [8].

VBM in normal aging

Studying the distribution and time course of alterations that occur in the normal brain with aging is important for understanding the mechanisms underlying these changes and for better characterization of neurological disorders whose risk increases with advancing age. The advent of VBM techniques of MRI structural data has facilitated a sensitive detection of regional patterns of gray matter and white matter volume changes. Most studies have employed a cross-sectional design in which correlations of volume and age at specific time points are used to make inferences about how the aging process affects the brain structure over time. However cross-sectional studies may inevitably have some degree of overlap of regional volume changes between normal aging and AD [9]. Large longitudinal VBM studies involving the acquisition of serial MRI measurements over time are desirable in the same subject samples [10].

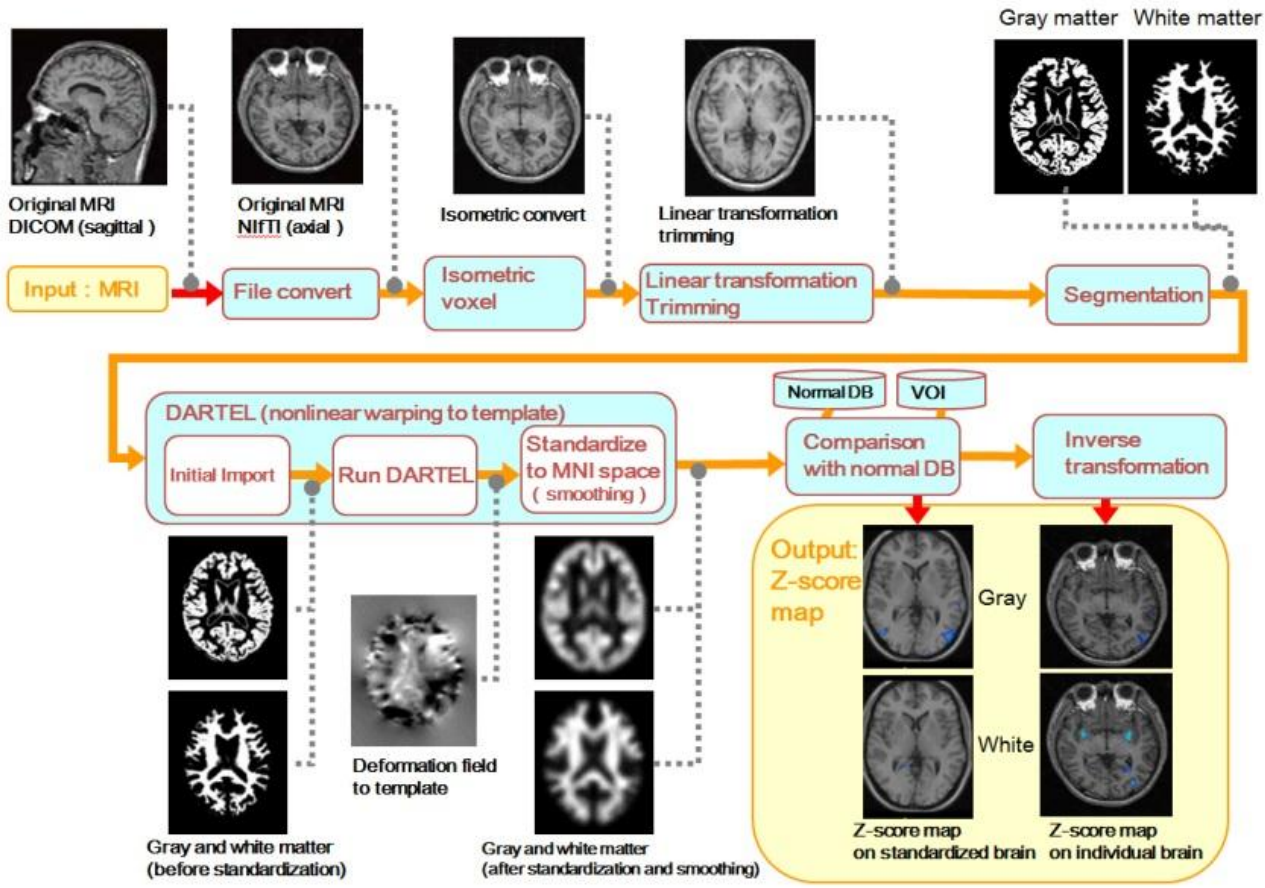

Figure 3. Procedure of stand-alone VBM software, VSRAD. Comparison of patient's MRI with MRI normal database yields color-coded Z-score maps of both gray matter and white matter using VBM analysis based on SPM8 plus DARTEL.

There have been a lot of VBM investigations on gray matter volume changes with advancing age (Table 1, Fig.1). Most cortical regions prominently in frontal and insular areas have been reported to show a linear negative association between volume and age [4,12-18]. In contrast, many reports have found preservation of gray matter volume in specific structures such as amygdala, hippocampus, and thalamus [4,12,14,17,18]. Relative preservation of these subcortical limbic or paralimbic regions is consistent with the functional importance of the thalamo-limbic circuits in sensory integration, arousal, emotion, and memory. This preservation in areas with the early maturation may lend credence to the idea that later-maturing cortical regions are more vulnerable to age-related morphologic changes. These age-related features may be already present during earlier stages of adulthood. During non-elderly life prefrontal areas showed linear volume reduction with advancing age, while medial temporal region showed volume preservation [18]. Cortical gray matter volume showed age-related reduction even during adolescence [19].

Throughout adulthood, white matter volumes also showed a linear negative association with advancing age in anterior thalamic radiation, internal capsule, cerebral peduncle, cerebellum, and external capsule [20](Fig.1). In contrast, nonlinear relationships between white matter volume and age were found in superior longitudinal fascicle and superior corona radiata. This nonlinear inverted U-shaped relationship with age, slightly increasing during adulthood, is consistent with the notion of an ongoing maturation of the white matter beyond adolescence, reaching its peak in the fourth decade.

In a longitudinal study of an interval of 2.5 years during adolescence, a significant increase in white matter was found in the frontal white matter bilaterally connected via the body of the corpus callosum [19]. In this context it must be remembered that dehydration may induce a significant widespread loss of white matter volume in the temporo-parietal areas [21]. Consequently,

VBM studies investigating white matter changes should consider controlling subjects' hydration state to avoid the potential confounder of differences in hydration.

The morphology of cortical gray matter is assessed using not only VBM but also cortical thickness measures. How gray matter changes identified using voxel-based cortical thickness measures compare with local gray matter volume changes identified using VBM was investigated [22]. VBM and voxel-based cortical thickness measures yield overall consistent results when investigating healthy aging but voxel-based cortical thickness provides a more sensitive measure of age-associated decline in gray matter compared with VBM. Voxel-based cortical thickness specifically measures cortical thickness, while VBM provides a mixed measure of gray matter including cortical surface area or cortical folding as well as cortical thickness.

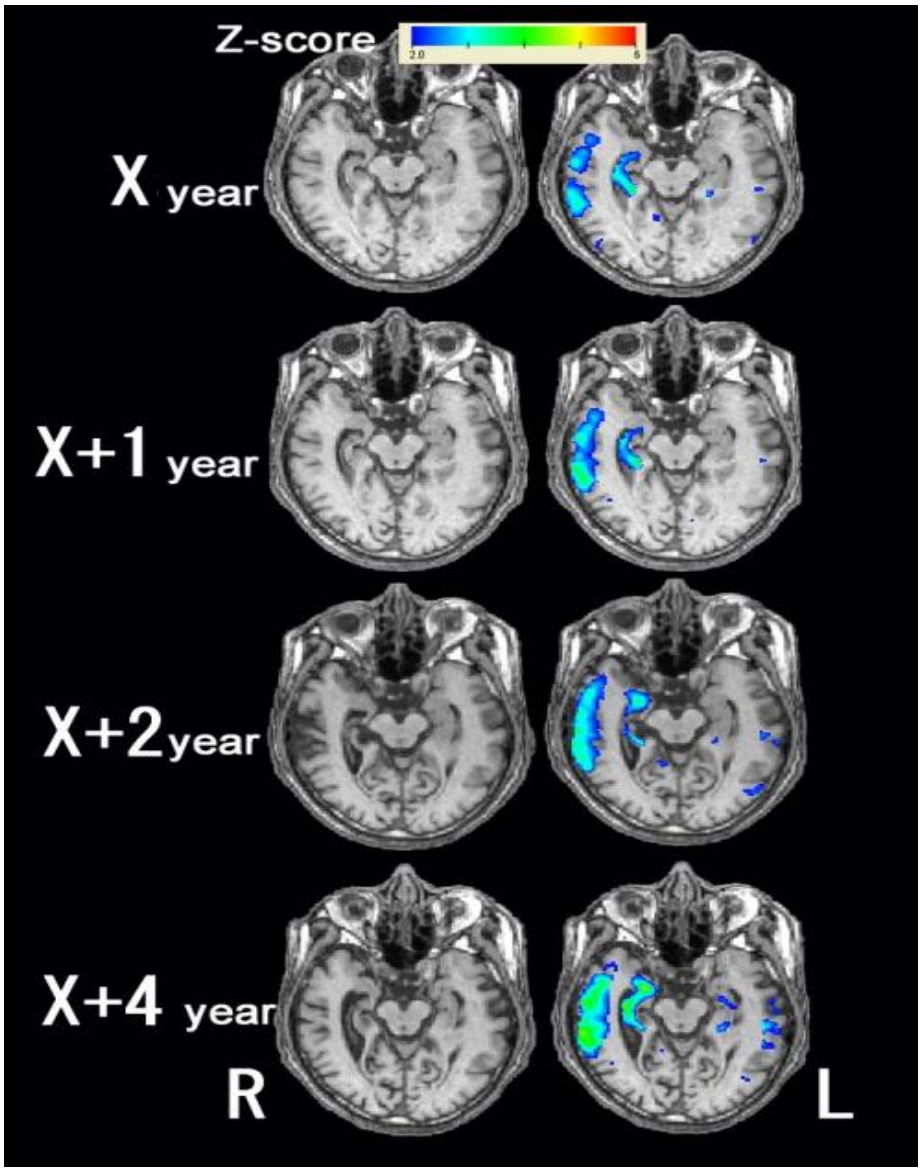

Figure 4. Longitudinal VBM analysis using VSRAD in a patient with AD. VSRAD demonstrates progressive atrophy in right-side dominant gray matter atrophy in medial and lateral temporal areas during a 5-year period in a man with AD aged 62 years at onset. Mini-mental state examination score decreased from 24 to 13 during this period. The severity, extent, ratio for the atrophy of medial temporal structures as the target VOI and the extent of whole brain atrophy are 1.3, 20.9%, 4.8, 3.8% at X year, 1.4,22.6%,5.8,4.3% at X+1 year, 1.6, 33.7%,6.2,5.4% at X+2 year, 2.4,55.1%, and 6.4, 8.5% at X+4 year, respectively.

VBM in Alzheimer's disease

Structural MRI measurements of brain atrophy are promising biomarkers for tracking disease progression in patients with AD. Progression of atrophy matches the stereotypical pattern of an increase in neurofibrillary tangles described by the Braak staging scheme [23]. Six stages are reported in the development of neurofibrillary tangles. Stages I and II involve the transentorhinal region which is situated along the lateral border of the entorhinal cortex and mediates between the entorhinal allocortex and temporal neocortex. The entorhinal region is located between the hippocampus and transentorhinal region, spreading over both the ambient gyrus and anterior portions of the parahippocampal gyrus. The brain change remains below the threshold associated with clinical symptoms. Stages III and IV severely involve both the entorhinal and transentorhinal regions accompanied by mild changes in the hippocampus and the virtual absence of changes in the neocortical regions. The clinical protocols of many individuals at these stages note an impairment of cognitive functions. Stages V and VI involve neocortical association areas. These stages correspond to the conventionally used criteria for neuropathologic confirmation of the clinical diagnosis of AD. Many researchers have demonstrated progression of atrophy in AD corresponding to these Braak stages using VBM [24-34] (Fig.2). In the Alzheimer's Disease Neuroimaging Initiative (ADNI) study [35], VBM showed strong associations between composite scores of memory generated from ADNI's neuropsychological battery and gray matter atrophy in the medial and lateral temporal lobes, and between composite scores of executive functions and gray matter atrophy in the parietal and temporal lobes.

Recent ante-mortem VBM studies [36] in demented patients with AD pathology revealed three subtypes based on the distribution of neurofibrillary tangles: typical AD, hippocampal-sparing AD, and limbic-predominant AD. Compared with typical AD, hippocampal-sparing AD has more neurofibrillary tangles and atrophy in the cortex and fewer in the hippocampus, whereas the opposite pattern is seen in limbic-predominant AD. Age at onset differed between subtypes, with the youngest ages recorded in the group with hippocampal-sparing AD and oldest in the group with limbic-predominant AD. This difference well explains why patients with early-onset AD have atypical clinical syndromes associated with widespread involvement in the association cortex. The topographical differences in gray matter involvement between early and late onset AD have been also reported by several investigators [37-39]

White matter changes have been reported to be less than gray matter changes in AD. Meta-analysis of VBM studies of white matter volume alterations in AD revealed significant volume reductions in the left parahippocampal gyrus extending to the temporal white matter, the right temporal white matter extending to the parahippocampal gyrus and posterior corpus callosum [40]. These white matter volume reductions are close to the structures of memory formation including the hippocampus, amygdala, and entorhinal cortex. The mechanism underlying white matter atrophy in AD remains unclear. There is one argument that gray matter degeneration results in white matter atrophy through demyelination because these regions contain efferent connections of both the hippocampus and amygdala. Another argument is that a white matter deficit contributes to the development of cortical pathology in AD. White matter damage in AD results in cortico-cortical and/or cortico-subcortical disconnection of cognitive networks and thus contributes to cognitive impairment in AD patients.

Voxel-based Specific Analysis System for Alzheimer's disease (VSRAD); VBM approach has been reported to show higher accuracy in discriminating AD and controls than VOI based analysis [41]. To facilitate VBM approach in an individual subject, a stand-alone software program running on Windows for VBM analysis based on SPM8 plus DARTEL was developed to discriminate a patient from healthy controls [42](Fig.3). First, MRI data were anatomically standardized with only 12-parameter affine transformation to the SPM template so as to correct for differences in brain size. Then MR images were segmented into gray matter, white matter, and CSF images by unified tissue segmentation procedure after image intensity nonuniformity correction. These linearly transformed and segmented images were nonlinearly transformed by DARTEL procedures and then modulated to the customized template for DARTEL followed by smoothing using an 8-mm FWHM kernel. Each processed segmented image was compared to the mean and standard deviation of gray matter or white matter images of the 80 healthy volunteers using voxel-by-voxel Z-score analysis with and without voxel normalization to global mean intensities (global normalization), Z-score=([control mean]-[individual value])/(control standard deviation). These Z-score maps were displayed by overlay on tomographic sections and surface rendering of the standardized brain. Inversed warping also makes it possible to display Z-score maps on the tomographic sections of the individual brain. This program registered the target VOI in medial temporal structures defined by group comparison of patients with early AD and healthy controls. This software program

takes approximately 9 min for all procedures using a 64-bit personal computer with Intel ® Core™ i7 CPU, 3.33 GHz, 6 gigabyte memory.

Four indicators for characterizing atrophy in the target VOI and in the whole brain were determined. The first is the severity of atrophy obtained from the averaged positive Z-score in the target VOI. The second is the extent of a region showing significant atrophy in the target VOI, that is, the percentage rate of the coordinates with a Z value exceeding the threshold value of 2 in the target VOI. The third is the extent of a region showing significant atrophy in the whole brain, that is, the percentage rate of the coordinates with a Z value exceeding the threshold value of 2 in the whole brain. These three indicators of severity and extent for the target VOI and extent for the whole brain are useful for early detection and longitudinal evaluation of AD (Fig.4). The fourth is the ratio of the extent of a region showing significant atrophy in the target VOI to the extent of a region showing significant atrophy in the whole brain. This ratio may be useful for differentiation of AD from other neuropsychiatric diseases manifesting dementia.

Conclusion

Progress has been made on VBM technique, and VSRAD software has been applied to routine clinical studies on AD in Japan. Atrophy rates of whole-brain and medial temporal structures are sensitive markers of neurodegeneration, and are increasingly being used as outcome measures in trials of potentially disease-modifying therapies. The utility of VBM will be increased hereafter as adjuncts to clinical assessment in the diagnosis and monitoring of progression of AD.

Acknowledgment

This work was supported by a Grant-in-Aid for Scientific Research (C), Ministry of Education, Culture, Sports, Science and Technology, Japan (24591786).

References

[1] Frisoni GB, Fox NC, Jack CR Jr, Scheltens P, Thompson PM (2010) The clinical use of structural MRI in Alzheimer disease. Nat Rev Neurol, 6:67-77.

[2] Ashburner J, Friston KJ (2000). Voxel-based morphometry--the methods. Neuroimage, 11:805-21.

[3] Ashburner J, Friston KJ (2001).Why voxel-based morphometry should be used. Neuroimage, 14:1238-43.

[4] Good CD, Johnsrude IS, Ashburner J, Henson RN, Friston KJ, Frackowiak RS (2001). A voxel-based morphometric study of ageing in 465 normal adult human brains. Neuroimage, 14:21-36.

[5] Karas GB, Burton EJ, Rombouts SA, van Schijndel RA, O'Brien JT, Scheltens P, et al. (2003). A comprehensive study of gray matter loss in patients with Alzheimer's disease using optimized voxel-based morphometry. Neuroimage, 18:895-907.

[6] Ashburner J (2007). A fast diffeomorphic image registration algorithm. Neuroimage, 38:95-113.

[7] Eggert LD, Sommer J, Jansen A, Kircher T, Konrad C (2012). Accuracy and reliability of automated gray matter segmentation pathways on real and simulated structural magnetic resonance images of the human brain. PLoS One,7:e45081.

[8] Klein A, Andersson J, Ardekani BA, Ashburner J, Avants B, Chiang MC, et al. (2009). Evaluation of 14 nonlinear deformation algorithms applied to human brain MRI registration. Neuroimage,46:786-802.

[9] Raji CA, Lopez OL, Kuller LH, Carmichael OT, Becker JT(2009). Age, Alzheimer disease, and brain structure. Neurology, 73:1899-905.

[10] Raz N, Lindenberger U, Rodrigue KM, Kennedy KM, Head D, Williamson A, et al.(2005). Regional brain changes in aging healthy adults: general trends, individual differences and modifiers, 15:1676-89.

[11] Resnick SM, Pham DL, Kraut MA, Zonderman AB, Davatzikos C (2003). Longitudinal magnetic resonance imaging studies of older adults: a shrinking brain. J Neurosci, 23:3295-301.

[12] Matsuda H, Ohnishi T, Asada T, Li ZJ, Kanetaka H, Imabayashi E, et al. (2003). Correction for partial-volume effects on brain perfusion SPECT in healthy men. J Nucl Med,44:1243-52.

[13] Tisserand DJ, van Boxtel MP, Pruessner JC, Hofman P, Evans AC, Jolles J (2004). A voxel-based morphometric study to determine individual differences in gray matter density associated with age and cognitive change over time. Cereb Cortex, 14:966-73.

[14] Grieve SM, Clark CR, Williams LM, Peduto AJ, Gordon E (2005). Preservation of limbic and paralimbic structures in aging. Hum Brain Mapp, 25:391-401.

[15] Smith CD, Chebrolu H, Wekstein DR, Schmitt FA, Markesbery WR (2007). Age and gender effects on human brain anatomy: a voxel-based morphometric study in healthy elderly. Neurobiol Aging, 28:1075-87.

[16] Curiati PK, Tamashiro JH, Squarzoni P, Duran FL, Santos LC, Wajngarten M, et al. (2009). Brain structural variability due to aging and gender in cognitively healthy Elders: results from the Sao Paulo Ageing and Health study. AJNR Am J Neuroradiol, 30:1850-6.

[17] Kalpouzos G, Chételat G, Baron JC, Landeau B, Mevel K, Godeau C, et al.(2009). Voxel-based mapping of brain gray matter volume and glucose metabolism profiles in normal aging. Neurobiol Aging,30:112-24.

[18] Terribilli D, Schaufelberger MS, Duran FL, Zanetti MV, Curiati PK, Menezes PR, et al. (2011). Age-related gray matter volume changes in the brain during non-elderly adulthood. Neurobiol Aging, 32:354-68.

[19] Giorgio A, Watkins KE, Chadwick M, James S, Winmill L, Douaud G, et al. (2010). Longitudinal

changes in grey and white matter during adolescence. Neuroimage, 49:94-103.

[20] Giorgio A, Santelli L, Tomassini V, Bosnell R, Smith S, De Stefano N, et al. (2010). Age-related changes in grey and white matter structure throughout adulthood. Neuroimage, 51:943-51.

[21] Streitbürger DP, Möller HE, Tittgemeyer M, Hund-Georgiadis M, Schroeter ML, Mueller K (2012). Investigating structural brain changes of dehydration using voxel-based morphometry. PLoS One, 7:e44195.

[22] Hutton C, Draganski B, Ashburner J, Weiskopf N (2009). A comparison between voxel-based cortical thickness and voxel-based morphometry in normal aging. Neuroimage, 48:371-80.

[23] Braak H, Braak E (1995). Staging of Alzheimer's disease-related neurofibrillary changes. Neurobiol Aging,16:271-8.

[24] Ohnishi T, Matsuda H, Tabira T, Asada T, Uno M (2001). Changes in brain morphology in Alzheimer disease and normal aging: is Alzheimer disease an exaggerated aging process? AJNR Am J Neuroradiol, 22:1680-5.

[25] Matsuda H, Kitayama N, Ohnishi T, Asada T, Nakano S, Sakamoto S, et al. (2002). Longitudinal evaluation of both morphologic and functional changes in the same individuals with Alzheimer's disease. J Nucl Med,43:304-11.

[26] Chetelat G, Desgranges B, de la Sayette V, Viader F, Berkouk K, Landeau B, et al. (2003). Dissociating atrophy and hypometabolism impact on episodic memory in mild cognitive impairment. Brain, 126:1955-67.

[27] Rémy F, Mirrashed F, Campbell B, Richter W (2005). Verbal episodic memory impairment in Alzheimer's disease: a combined structural and functional MRI study. Neuroimage,25:253-66.

[28] Hirata Y, Matsuda H, Nemoto K, Ohnishi T, Hirao K, Yamashita F, et al. (2005). Voxel-based morphometry to discriminate early Alzheimer's disease from controls. Neurosci Lett,382:269-74.

[29] Di Paola M, Macaluso E, Carlesimo GA, Tomaiuolo F, Worsley KJ, Fadda L, et al. (2007). Episodic memory impairment in patients with Alzheimer's disease is correlated with entorhinal cortex atrophy. A voxel-based morphometry study. J Neurol, 254:774-81.

[30] Hämäläinen A, Pihlajamäki M, Tanila H, Hänninen T, Niskanen E, Tervo S, et al. (2007). Increased fMRI responses during encoding in mild cognitive impairment. Neurobiol Aging, 28:1889-903.

[31] Leube DT, Weis S, Freymann K, Erb M, Jessen F, Heun R, et al. (2008). Neural correlates of verbal episodic memory in patients with MCI and Alzheimer's disease--a VBM study. Int J Geriatr Psychiatry,23:1114-8.

[32] Schmidt-Wilcke T, Poljansky S, Hierlmeier S, Hausner J, Ibach B (2009). Memory performance correlates with gray matter density in the ento-/perirhinal cortex and posterior hippocampus in patients with mild cognitive impairment and healthy controls--a voxel based morphometry study. Neuroimage, 47:1914-20.

[33] Goto M, Abe O, Miyati T, Yoshikawa T, Hayashi N, Takao H, et al. (2011). Entorhinal cortex volume measured with 3T MRI is positively correlated with the Wechsler Memory Scale-Revised logical/verbal memory score for healthy subjects. Neuroradiology, 53:617-22.

[34] Chételat G, Villemagne VL, Pike KE, Ellis KA, Bourgeat P, Jones G, et al. (2011). Independent contribution of temporal beta-amyloid deposition to memory decline in the pre-dementia phase of Alzheimer's disease. Brain, 134:798-807.

[35] Nho K, Risacher SL, Crane PK, Decarli C, Glymour MM, Habeck C, et al.(2012). Voxel and surface-based topography of memory and executive deficits in mild cognitive impairment and Alzheimer's disease. Brain Imaging Behav, DOI 10.1007/s11682-012-9203-2

[36] Whitwell JL, Dickson DW, Murray ME, Weigand SD, Tosakulwong N, Senjem ML, et al. (2012). Neuroimaging correlates of pathologically defined subtypes of Alzheimer's disease: a case-control study. Lancet Neurol,11:868-77.

[37] Ishii K, Kawachi T, Sasaki H, Kono AK, Fukuda T, Kojima Y,et al. (2005). Voxel-based morphometric comparison between early- and late-onset mild Alzheimer's disease and assessment of diagnostic performance of z score images. AJNR Am J Neuroradiol, 26:333-40.

[38] Matsunari I, Samuraki M, Chen WP, Yanase D, Takeda N, Ono K et al. (2007). Comparison of ^{18}F-FDG PET and optimized voxel-based morphometry for detection of Alzheimer's disease: aging effect on diagnostic performance. J Nucl Med, 2007;48:1961-70.

[39] Frisoni GB, Pievani M, Testa C, Sabattoli F, Bresciani L, Bonetti M, et al.(2007). The topography of grey matter involvement in early and late onset Alzheimer's disease. Brain, 2007;130:720-30.

[40] Li J, Pan P, Huang R, Shang H (2012). A meta-analysis of voxel-based morphometry studies of white matter volume alterations in Alzheimer's disease. Neurosci Biobehav Rev,36:757-63.

[41] Testa C, Laakso MP, Sabattoli F, Rossi R, Beltramello A, Soininen H, et al.(2004). A comparison between the accuracy of voxel-based morphometry and hippocampal volumetry in Alzheimer's disease. J Magn Reson Imaging,19:274-82.

[42] Matsuda H, Mizumura S, Nemoto K, Yamashita F, Imabayashi E, Sato N, et al. (2012). Automatic voxel-based morphometry of structural MRI by SPM8 plus diffeomorphic anatomic registration through exponentiated lie algebra improves the diagnosis of probable Alzheimer Disease. AJNR Am J Neuroradiol,33:1109-14.